Fundamental Limits of Electronic Signal Processing in Direct-Detection Optical Communications

Michele Franceschini, Giorgio Bongiorni, Gianluigi Ferrari, *Member, IEEE*,
Riccardo Raheli, *Member, IEEE*, Fausto Meli, and Andrea Castoldi

Abstract—Electronic signal processing is becoming very attractive to overcome various impairments that affect optical communications, and electronic dispersion compensation (EDC) represents a typical application in the currently designed systems. However, the inherent limits in performance achievable by electronically processing the signal at the output of a nonlinear photodetector have not received the attention they deserve. In this paper, we investigate the information-theoretic limits of electronic signal processing in transmission systems employing direct photodetection and two possible modulation formats: 1) on–off keying (OOK) with nonreturn-to-zero pulses; and 2) optical duobinary modulation (ODBM). The analysis is based on the computation of the information rate, i.e., the maximum achievable data transfer rate, and accounts for the modulation format as well as relevant parameters of the transmission scheme. In particular, we investigate the impact of sampling rate, uncompensated chromatic dispersion (CD), and quantization resolution of the electrical signal at the output of a direct photodetector. For OOK systems, the obtained results show that the optical signal-to-noise ratio penalty entailed by EDC can be limited to about 2 dB at most values of CD of interest in current applications. Moreover, ODBM systems at high values of CD can almost perform as OOK systems at zero CD. For all the considered modulation formats, the obtained results show that the received electrical signal can be sampled at a rate of two samples per bit interval and quantized with a precision of 3 bits per sample to practically achieve the ultimate performance limits.

Index Terms—Direct photodetection, electronic dispersion compensation (EDC), information rate, maximum-likelihood sequence detection (MLSD), on–off keying (OOK), optical duobinary modulation (ODBM), quantization.

I. INTRODUCTION

DUE TO the decreasing cost of powerful integrated circuits, electronic signal processing in digital optical communication systems is receiving increasing scientific and industrial interest. In 10-Gb/s optical links such as those used in metropolitan and wide area networks, chromatic dispersion (CD) is a relevant physical phenomenon that must be dealt with. Precompensation techniques at the transmitter side or dispersion compensation techniques at the receiver side can be used [1]. Electronic dispersion compensation (EDC) is a particular instance of electronic signal processing designed to combat uncompensated CD effects [2]. The corresponding signal processing can be performed by means of analog or digital electronic techniques, although the latter is of preeminent interest today. EDC can be an appealing solution that can lead to replace (or reduce) costly optical dispersion compensation units, guarantee robustness, and enable system adaptivity.

Several EDC solutions have been proposed in the literature, the most important of which are: 1) electronic equalization [2]–[5]; and 2) maximum-likelihood sequence detection (MLSD)[1] [2], [6]–[11]. These techniques enable enhanced detection performance at the receiver. In particular, MLSD allows detection of the transmitted sequence with minimum probability of error and therefore represents an important benchmark for the performance achievable by EDC. Nevertheless, the performance obtained by MLSD does not represent the ultimate achievable performance limit, since it depends on the particular choice of the channel coding/modulation scheme (although, in the literature, the interaction between coding and modulation is typically neglected, and uncoded schemes are usually investigated).

Two useful quantities characterizing a transmission channel are: 1) the *information rate* (IR), which corresponds to the maximum transfer rate that can be reliably achieved by practical transmission schemes, with a specific modulation format [12]; and 2) the *channel capacity*, which corresponds to the supremum of the IR of the channel, considering optimized data source statistics and modulation format. IR and capacity therefore allow to tackle the problem of performance characterization of the optical communication systems of interest. In practice, however, there are two advantages in designing communications systems considering the IR instead of the capacity.

1) The capacity of a channel is typically very difficult to evaluate, and only approximations are available. On the opposite, efficient techniques exist for accurate computation of the IR [13]–[16].
2) In usual scenarios, engineering constraints allow to choose among a rather small set of modulation formats and channel input distributions such as, for example, on–off keying (OOK) or optical duobinary modulation (ODBM) [1], [17]. In these cases, the IR is the significant performance indicator since, due to design constraints, the optimization over the channel input distribution is of limited practical interest.

[1]Strictly speaking, MLSD systems attempt neither to *compensate* the chromatic dispersion effects nor to equalize them, but duly account for these effects in the data detection process.

Fig. 1. Optical communication system model with direct photodetection.

In the literature, several papers dealing with the *capacity* of fiber-optic channels have appeared, among which [18]–[20]. In [21], Shamai derives upper and lower bounds on the capacity of the optical fiber channel with direct photodetection. The considered channel is characterized by a very low received photon rate, and the approach for the computation of capacity exploits the discrete nature of the observed process. In [22], the binary-input IR and channel capacity of an optical link is investigated considering a perfectly compensated (i.e., memoryless) optical transmission scheme. In [22], it is also shown how to achieve a performance close to the IR limit through modern coding techniques (such as, for example, turbo codes [23]). In [24], the authors use the IR for performance characterization of long-haul optical links. The analysis in [24] is based on the method proposed in [13]–[16] and takes into account several linear and nonlinear effects of optical fibers. The channel characterization method is based on a Monte Carlo evaluation of the statistical parameters of a long-haul optical link. The authors consider OOK with bit-rate (or *synchronous*) sampling, and the IR is evaluated as a function of the number of spans and launched power.

In this paper, we evaluate the IR of an optical fiber communication system with direct photodetection impaired by moderate and severe CD. Our goal is to investigate the ultimate attainable performance limit of EDC or, more generally, of *electronic signal processing*. The IR is evaluated in the presence of different modulation formats suitable for direct photodetection, which are 1) OOK with nonreturn-to-zero (NRZ) pulses and 2) ODBM. The fiber is affected by CD and white Gaussian amplified spontaneous emission (ASE) noise. The exact statistical distribution of the observed electrical signal derived in [25] is exploited to compute a tight lower bound on the IR as a function of the optical signal-to-noise ratio (OSNR). The IR sensitivity to sampling epoch and the sampling rate needed to achieve good performance are investigated: we show that two samples per bit interval are needed to effectively cope with CD in the electrical domain. The impact of quantization is also addressed, and the tradeoff between the number of bits used to represent the received signal and the system performance is investigated: a quantization rate of 3 bits per sample is sufficient to practically recover all the information contained in the received electrical signal. Numerical results are shown in terms of both IR (as a function of the OSNR for a given value of CD) and OSNR (as a function of the uncompensated CD), which are required to achieve a desired value of IR. In particular, we fix the IR at the rate of a typical Reed–Solomon (RS) forward error correction (FEC) code [26]. In the considered communication scenario with NRZ OOK signaling, we show that the theoretical OSNR penalty with respect to a scenario

with no dispersion (*back-to-back*, B2B) is at most 2 dB at CD values of up to 10 000 ps/nm, which corresponds, e.g., to a haul of about 600 km of a typical single-mode fiber. In the case of ODBM, a good performance can be achieved in the medium/high-dispersion region with performance *gains* with respect to a B2B scenario of more than 2 dB. In addition, our results suggest that the OSNR penalty exhibits an asymptotic convergence for increasing values of CD, especially in the case of NRZ OOK. In other words, for larger and larger values of CD, the OSNR penalty saturates. The results presented in this paper expand upon [27], where the impact of CD on the performance of an NRZ OOK transmission scheme was briefly addressed. We remark that, although the considered fiber model is linear, the adopted method can be extended to account for fiber nonlinearity and to investigate other modulation formats such as, for example, carrier-suppressed return-to-zero modulation or differential phase-shift keying [28].

This paper is outlined as follows. In Section II, the considered communication system models are described. In Section III, the IR computation technique is reviewed, and the peculiarities of the considered transmission schemes are discussed. In Section IV, a technique for low-complexity accurate evaluation of the channel statistics needed in the computation of the IR is introduced. In Section V, the parameters characterizing the considered communication schemes are shown. In Section VI, the impact of sampling rate on the IR is investigated. In Section VII, the performance with and without quantization of the received signal is investigated considering both NRZ OOK and ODBM. In Section VIII, the obtained numerical results are discussed. Section IX concludes this paper.

II. COMMUNICATION SYSTEM MODEL

As mentioned in Section I, we consider two different optical modulation schemes, which are 1) OOK with NRZ pulses and 2) ODBM. In Fig. 1, an optical communication system model with direct photodetection is shown. At the input of the system, a sequence of independent and equally likely information bits $\mathcal{A}$ is considered. In the OOK case, the modulator (MOD) comprises an NRZ pulse shaping filter, an electrical low-pass filter, and a Mach–Zehnder device. The input/output relation of the Mach–Zehnder device is

$$E_{\text{out}} = E_0 \cos\left(\frac{\pi}{4} + \mu\frac{\pi}{2}V_{\text{in}}\right) \tag{1}$$

where E_{out} is the output electrical field, E_0 is the input electrical field from the laser source, μ is the modulation index, and V_{in} is the input voltage normalized in the range $(-0.5, 0.5)$.

The modulated signal propagates through a linear optical fiber modeled by the frequency response [1]

$$H_{\text{fiber}}(f) = e^{-jDz\frac{\pi\lambda^2}{c}f^2} \quad (2)$$

where D is the CD factor (dimension: [ps/nm km], z is the distance (dimension: [km]), Dz is the total amount of uncompensated CD (dimension: [ps/nm]), λ is the optical carrier wavelength (dimension: [nm]), and c is the speed of light ($c \simeq 3 \times 10^5$ km/s). The received optical signal is corrupted by wideband ASE noise, which is characterized by polarization components both parallel and orthogonal to that of the useful signal. The ASE noise is modeled as a white Gaussian complex bidimensional vector process (one complex dimension per polarization) [1]. The monolateral power spectral density per complex dimension is N_0. The received optical signal, i.e., the sum of useful signal and noise, is filtered by an optical filter with transfer function $H_o(f)$ and then converted to an electrical signal by a square-law photodetector. The signal is then filtered by an electrical filter with transfer function $H_e(f)$.

The obtained electrical signal $y(t)$ is sampled at frequency $f_s = \eta/T_b$, where T_b is the bit interval, and η is the sampling rate expressed in samples per bit interval (or oversampling factor). For simplicity, only integer values of η are considered. The samples are collected in vectors $y_k = (y_k^{(0)}, \ldots, y_k^{(\eta-1)}) = (y(t_k^{(0)}), \ldots, y(t_k^{(\eta-1)}))$ of η elements representing the actual output of the channel at the instants

$$t_k^{(i)} = \left(k + \frac{i}{\eta}\right)T_b + \tau_0 + \tau, \quad \text{for } i = 0, \ldots, \eta - 1 \quad (3)$$

where τ_0 is used to align the information sequence and the output sample sequence accounting for the delay introduced by the various blocks in the communication system, k is the running bit-time index, i scans the bit interval by multiples of T_b/η, and τ denotes the sampling offset or *epoch*. The output time-discrete process, which is denoted as $\mathcal{Y}$, can be inputted to an electronic signal processing device, such as an EDC unit. We will not discuss the internal structure of this device since our focus is on the ultimate theoretical performance achievable by EDC that by its own spirit is independent of the specific implementation of the EDC device.

The scheme in Fig. 1 can be used to represent an ODBM communication system model as well. The system structure is basically the same as for the NRZ OOK system. The only difference is in the modulation block and consists of the following: 1) the presence of a precoder, which is inserted in ODBM transmission schemes to enable simple threshold detection at the receiver [17]; and 2) a different input–output characteristic of the Mach–Zehnder device. The precoder consists of a modulo-2 accumulator encoding the input information bits into transitions in the binary sequence at the input of the ODBM modulator. As we will see, the presence of the precoder modifies the memory structure of the overall transmission scheme and must be properly taken into account. The Mach–Zehnder device input–output relation in the ODBM case is

$$E_{\text{out}} = E_0 \cos\left(\frac{\pi}{2} + \pi V_{\text{in}}\right) \quad (4)$$

where E_{out} is the output electrical field, E_0 is the input electrical field from the laser source, and V_{in} is the input voltage normalized in the range $(-0.5, 0.5)$.

The sources of memory in the channel models shown in Fig. 1 are the modulation filters at the transmitter side, the fiber, the optical and electrical filters in the receiver front end, and, only in the case of ODBM, the precoder. As common practice in detection theory, we define the *overall channel memory* as L, with $L + 1$ corresponding to the number of (consecutive) bits, including the current one, which influence a particular observable [29]. Formally, the joint probability density function (pdf) of the observable vector y_k at the kth signaling interval satisfies a finite memory property [30]

$$p\left(y_k|y_0^{k-1}, a_0^{K-1}\right) = p\left(y_k|y_0^{k-1}, a_{k-L}^k\right) \quad (5)$$

where the notation a_l^p stands for the sequence of information bits given by $(a_l, a_{l+1}, \ldots, a_p)$, and K is the total number of transmitted bits. In other words, the observable y_k depends on $L + 1$ information bits. The above notation enables a compact representation that accounts for possible oversampling with respect to the bit rate. The special case of bit-rate (or synchronous) sampling is simply accounted for by letting $\eta = 1$. The only difference between these two cases is that y_k is a real scalar for $\eta = 1$ and an η-dimensional real vector for $\eta > 1$.

III. IR COMPUTATION

The discrete process $\mathcal{A}$ at the input of the transmission scheme consists of a sequence of independent and identically distributed binary random variables $\{a_k\}$ that take on values in the set $\{0, 1\}$ and are characterized by $P\{a_k = 0\} = P\{a_k = 1\} = 1/2$. The output of the transmission scheme, for the purpose of IR definition, is represented by the discrete-time process $\mathcal{Y}$. Under the assumption of joint ergodicity and stationarity of $\mathcal{A}$ and $\mathcal{Y}$, according to the Shannon–McMillan–Breiman theorem, the IR can be expressed as [12], [16]

$$I(\mathcal{A}; \mathcal{Y}) = \lim_{n \to \infty} \frac{1}{n} [-\log p(y_1, \ldots, y_n)$$
$$+ \log p(y_1, \ldots, y_n|a_1, \ldots, a_n)] \quad (6)$$

where $(y_1, \ldots, y_n)$ are n received (possibly vector) observables, and $(a_1, \ldots, a_n)$ are the corresponding information bits.

Since the overall memory of the transmission system is practically finite, it is possible to introduce a finite state machine (FSM) model of the transmission scheme with state s_k at the kth signaling interval. In particular, the FSM memory parameter L is a design parameter to be chosen large enough to make the model accurate. Since both the input process and the channel are ergodic, $\mathcal{A}$ and $\mathcal{Y}$ are jointly ergodic and stationary [31]. In the case of OOK, the state s_k^{ook} at the kth signaling interval is defined as

$$s_k^{\text{ook}} \triangleq (a_{k-L}, \ldots, a_{k-1})$$

i.e., it is a vector of L consecutive information bits. The alignment parameter τ_0 in (3) can be chosen in order to minimize L

while preserving the model accuracy. Assuming that the fiber transfer function is modeled noncausally as in (2) and that the optical and electrical filter impulse responses are short, i.e., less than T_b, an effective value for the alignment parameter is $\tau_0 = -T_b L/2$. In the case of ODBM, the presence of the recursive precoder suggests a proper redefinition of the state. In particular, we define the ODBM state as

$$s_k^{\text{odbm}} \triangleq (c_{k-L}, \ldots, c_{k-1}) \tag{7}$$

where $\{c_k\}$ is the sequence of precoded bits defined by the recursion

$$c_k = (a_k + c_{k-1}) \bmod 2.$$

According to (7), the state depends only on the binary symbols c_k that are actually processed by the modulator. This enables the use of the same formal model to describe the statistical dependence of the channel output on the FSM state for both OOK and ODBM.[2]

The IR can be computed by using the Monte Carlo approach proposed in [13]–[16]. More precisely, for a sufficiently large number n of consecutive observations, the exact IR in (6) can be approximated as

$$I(\mathcal{A}; \mathcal{Y}) \simeq \frac{1}{n} \left[-\log p(\boldsymbol{y}_1, \ldots, \boldsymbol{y}_n) \right.$$
$$\left. + \log p(\boldsymbol{y}_1, \ldots, \boldsymbol{y}_n | a_1, \ldots, a_n) \right] \tag{8}$$

where the pdf $p(\boldsymbol{y}_1, \ldots, \boldsymbol{y}_n)$ is obtained by means of a recursive computation based on the received samples $(\boldsymbol{y}_1, \ldots, \boldsymbol{y}_n)$, and the conditional pdf $p(\boldsymbol{y}_1, \ldots, \boldsymbol{y}_n | a_1, \ldots, a_n)$ can be computed analytically [25] or approximately as described in Section IV. In [13]–[16], the recursive computation of $p(\boldsymbol{y}_1, \ldots, \boldsymbol{y}_n)$ is shown to be equivalent to the forward recursion of a forward–backward algorithm [32] and is based on the knowledge of the generic conditional pdf $p(\boldsymbol{y}_k | \boldsymbol{y}_0^{k-1}, \boldsymbol{a}_0^n)$ of the observable $\boldsymbol{y}_k$. In practice, given the transmitted data sequence $\boldsymbol{a}_0^n$, the observable $\boldsymbol{y}_k$ depends only on a finite number γ of previous observables. Taking into account the finite memory condition (5), the conditional pdf can be expressed as

$$p\left(\boldsymbol{y}_k | \boldsymbol{y}_0^{k-1}, \boldsymbol{a}_0^n\right) = \begin{cases} p\left(\boldsymbol{y}_k | \boldsymbol{y}_{k-\gamma}^{k-1}, \boldsymbol{a}_{k-L}^k\right), & \text{for OOK} \\ p\left(\boldsymbol{y}_k | \boldsymbol{y}_{k-\gamma}^{k-1}, \boldsymbol{c}_{k-L}^k\right), & \text{for ODBM} \end{cases} \tag{9}$$

where the parameter $\gamma \in \mathbb{N}$ is the number of past observables on which $\boldsymbol{y}_k$ depends given the transmitted bit sequence. The

parameter γ is proportional to the system memory due to the front end that affects the ASE noise and can be effectively approximated by

$$\gamma \simeq \left\lfloor \frac{\sigma_o + \sigma_e}{T_b} + 1 - \frac{1}{\eta} \right\rfloor$$

where σ_o and σ_e are the root-mean-square duration of the optical and electrical filters, respectively [1], and the notation $\lfloor x \rfloor$ denotes the integer part, i.e., the largest integer less than or equal to x. In practical situations, $\gamma \in \{0, 1\}$, where $\gamma = 0$ means that the noise has a memory shorter than the sampling period, i.e., 1) there is no dependence of $\boldsymbol{y}_k$ on $\boldsymbol{y}_0^{k-1}$ given the sequence $\boldsymbol{a}_0^k$; and 2) there is no dependence of $y_k^{(i)}$ on $y_k^{(j)}$ for $i, j = 0, \ldots, \eta - 1$ and $i \neq j$. Values of γ larger than 1 would not be of practical interest since the only parameter influencing γ is the receiver front-end memory, which is usually kept as small as possible in order to avoid intersymbol interference. For $\eta > 1$ samples per bit interval, the pdf in (9) can be factored as (considering OOK)

$$p\left(\boldsymbol{y}_k | \boldsymbol{y}_{k-\gamma}^{k-1}, \boldsymbol{a}_{k-L}^k\right) = \prod_{i=0}^{\eta-1} p\left(y_k^{(i)} | y_k^{(i-1)}, \ldots, y_k^{(0)}, \boldsymbol{y}_{k-\gamma}^{k-1}, \boldsymbol{a}_{k-L}^k\right). \tag{10}$$

We point out that if the noise has a memory shorter than the sampling period, i.e., $\gamma = 0$, (10) becomes

$$p\left(\boldsymbol{y}_k | \boldsymbol{y}_{k-\gamma}^{k-1}, \boldsymbol{a}_{k-L}^k\right) = \prod_{i=0}^{\eta-1} p\left(y_k^{(i)} | \boldsymbol{a}_{k-L}^k\right). \tag{11}$$

In [25], a method for the exact evaluation of $p(y_k^{(i)} | \boldsymbol{a}_{k-L}^k)$ is proposed, which enables the computation of (11), i.e., (9) for $\gamma = 0$. In the following, we will assume $\gamma = 0$, and for the evaluation of the conditional pdf, we will use the method proposed in [25]. Since a conservative approach to channel modeling would account for the dependence between observables conditioned on the transmitted bit sequence, i.e., $\gamma = 1$, the assumption $\gamma = 0$ will lead to a mismatch between the actual channel and the channel model used for the evaluation of the pdfs. Unfortunately, a closed-form expression for (9) with $\gamma = 1$ is not available, and its statistical analysis is computationally prohibitive. On the other hand, extensive statistical analysis has shown that, in the considered scenarios, the typical correlation coefficient (conditioned on a particular bit sequence) between two samples at one half bit period distance (corresponding to two consecutive samples at $\eta = 2$) is about 0.1 with maximum peaks of about 0.2. Moreover, the correlation between samples, which are at a distance of 1 bit period, is negligible. This suggests that the approximation based on assuming $\gamma = 0$ is numerically accurate.

In [16], it is shown that if the received samples $\{\boldsymbol{y}_k\}$ are generated with the actual channel model, and the pdfs $p(\boldsymbol{y}_1, \ldots, \boldsymbol{y}_n)$ and $p(\boldsymbol{y}_1, \ldots, \boldsymbol{y}_n | a_1, \ldots, a_n)$ are computed using a different channel model, i.e., an "auxiliary channel," the obtained IR value is a lower bound on the actual IR. As a consequence, all the mismatches in channel modeling, among which the most important ones come from the assumptions that

---

[2]We remark that the state in (7) is equivalent to $(c_{k-L}, a_{k-L+1}, \ldots, a_{k-1})$. It is then possible to exploit the particular symmetry of ODBM to obtain a reduction of the state space. In fact, since the output of the square-law photodetector does not change upon a signal phase rotation, the states $(c_{k-L}, a_{k-L+1}, \ldots, a_{k-1})$ and $(-c_{k-L}, a_{k-L+1}, \ldots, a_{k-1})$ entail the same conditional pdf of the observable. In other words, there is no statistical dependence on c_{k-L}. The ODBM state can therefore be equivalently redefined as

$$s_k^{\text{odbm}} \triangleq (a_{k-L+1}, \ldots, a_{k-1}).$$

1) L is finite and 2) the observation samples are conditionally independent, contribute to an *underestimation* of the true IR. This fact will be taken into account in discussing the obtained results in terms of tight lower bounds.

IV. ACCURATE APPROXIMATION OF THE PDF OF THE OBSERVABLES

While the computation of the conditional pdf of the observation $y_k^{(i)}$ based on the techniques presented in [25] is *exact*, it does not lead to a simple closed-form expression for this pdf and therefore does not lend itself to a low-complexity evaluation. By heuristic considerations, we found that the following function can be used to accurately "fit" the exact pdf:

$$f(y) = \exp\left(a + by + cy^{\frac{1}{2}} + d\ln y\right) \qquad (12)$$

where a, b, c, and d are suitable parameters to be optimized in order to minimize the mean square error (MSE) between the exact pdf and $f(y)$. Obviously, the parameters a, b, c, and d depend on 1) the specific bit sequence; 2) the OSNR; and 3) the value of the dispersion and the other parameters affecting the overall transmission scheme.

In the numerical computation, we used MATLAB to derive the fitting parameters a, b, c, and d. In particular, we used an implementation of the Levenberg–Marquardt algorithm for nonlinear regression [33]. While the used fitting operation gives a very low MSE, two main issues are relevant.

1) The relative distance between exact and fitted curves becomes significant in the tails.
2) The nonlinear fitting algorithm is very complex.

These two issues can be solved by fitting the logarithm of the actual pdf with the logarithm of the function $f(y)$, i.e.,

$$\ln f(y) = a + by + cy^{\frac{1}{2}} + d\ln y. \qquad (13)$$

In this case, a linear minimum MSE (or least mean square, LMS) can be considered due to the linearity of the fitting function in the parameters a, b, c, and d. LMS represents an appealing solution due to its limited computational complexity.

In Fig. 2, a direct comparison between the exact pdf and the corresponding best-fit pdf is shown, which considers two possible transmission patterns $(a_{k-L}, \ldots, a_k) = (1,1,1,1,1)$ and $(a_{k-L}, \ldots, a_k) = (0,0,0,0,0)$, i.e., an all-"1" transmission pattern and an all-"0" transmission pattern, respectively. The considered modulation format is NRZ OOK, and the communication system is B2B. The FSM memory parameter is $L = 4$. Although a different system setup, i.e., different filters, modulation, OSNR, and CD, leads to a different pdf, the fitting procedure is highly accurate in all cases. The fact that the proposed fitting function is similar to the analytical approximation proposed in [11] indirectly confirms the validity of the proposed approach. We performed an extensive set of tests considering several bit patterns, OSNR, and CD values. The results show that there is an excellent agreement between the exact pdf and the proposed best-fit approximation. The approximation in (13)
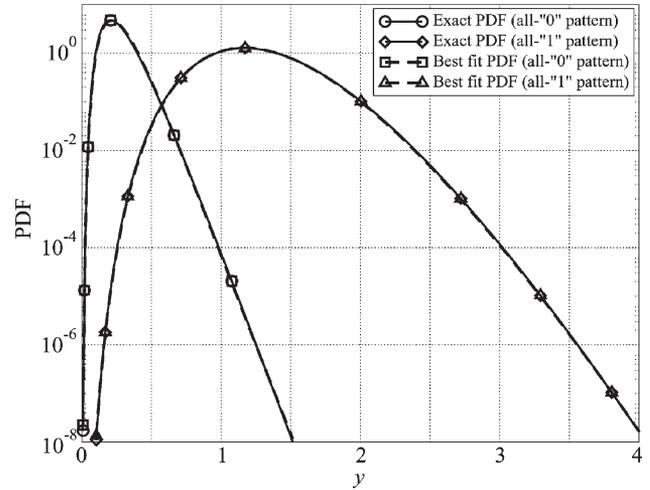
Fig. 2.   Direct comparison of the exact observable pdfs with their best fitting functions for an NRZ OOK system at B2B. An all-"1" transmission pattern, i.e., "ON-state," and an all-"0" transmission pattern, i.e., "OFF-state," are considered. The OSNR is 8 dB.

TABLE I
L AS A FUNCTION OF CD

CD [ps/nm]	0	1700	3400	6800	9350	10200
L	4	6	8	10	12	14

is a very accurate alternative to the approximate closed-form formulas found in [11] and [34].

V. ANALYSIS AND SIMULATION SETUP

In the following sections, we will consider two 10-Gb/s schemes with 1) NRZ OOK and 2) ODBM.

The OOK system setup is as follows. With reference to Fig. 1, the low-pass modulator electrical filter is a third-order Bessel filter with bandwidth of 9.5 GHz; the modulation index μ in (1) is equal to 0.93, which corresponds to an extinction ratio of 24.3 dB at the transmitter side; the optical filter is a third-order Bessel filter with bandwidth of 32.5 GHz; and the electrical filter is a fifth-order Bessel filter with bandwidth of 7.7 GHz.

The ODBM system setup is as follows. With reference to Fig. 1, the low-pass modulation electrical filter is a fifth-order Bessel filter with bandwidth of 3 GHz; the optical filter is a third-order Bessel filter with bandwidth of 33 GHz; and the electrical filter is a fifth-order Bessel filter with bandwidth of 7.7 GHz.

As discussed in Sections II and III, the memory L of the FSM that models the transmission scheme depends on its characteristics. In particular, the system memory L is an increasing function of the uncompensated CD value. The results in the following sections are obtained considering the conservative values of L indicated in Table I as a function of the CD. These values have been chosen to ensure convergence of the IR computation algorithm.
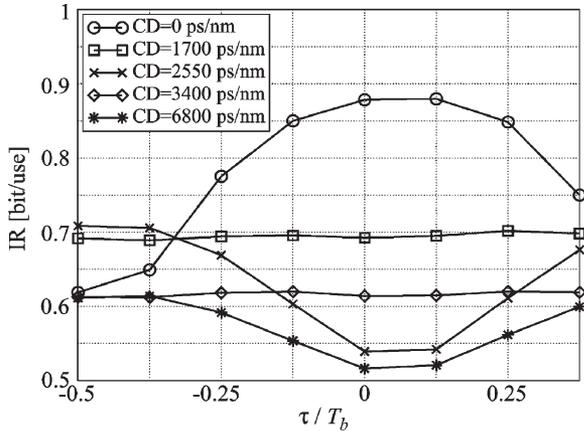
Fig. 3. IR as a function of the normalized sampling epoch τ/T_b in a scenario with $\eta = 1$ sample per bit interval and OSNR equal to 6 dB.

Fig. 4. IR as a function of OSNR at dispersion values of 0, 1700, 3400, and 6800 ps/nm, respectively. In all cases, values of η equal to one and two samples per bit interval are considered.

In all the following results, the OSNR is defined as the ratio between the average received signal power and the noise power in a bandwidth corresponding to 0.1 nm with carrier wavelength equal to 1550 nm.

VI. IMPACT OF SAMPLING RATE AND EPOCH

In this section, we investigate the effects of the sampling epoch and rate on the IR and therefore on the maximum attainable data transfer rate. The results presented in this section refer to a scenario with OOK. However, similar results can be obtained considering ODBM. The IR has been evaluated, according to the approach proposed in Section III, by Monte Carlo simulations based on sequences of $n = 10^6$ information bits.

In Fig. 3, a lower bound on the IR is shown as a function of the normalized sampling epoch τ/T_b in a scenario with OSNR equal to 6 dB and $\eta = 1$ sample per bit interval. CD values equal to 0, 1700, 2550, 3400, and 6800 ps/nm are considered. The value $\tau = 0$ corresponds to a reference sampling epoch determined by transmitting a single pulse (a single "1") at zero dispersion (i.e., in B2B) and observing the instant at which the signal at the output of the electrical filter reaches its peak. One can observe that, while $\tau = 0$ is almost optimal for a CD equal to 0 ps/nm, at some values of CD (1700 and 3400 ps/nm), there is no dependence on the sampling epoch τ, and at other values of CD (2550 and 6800 ps/nm), the optimum sampling epoch is $\tau = -0.5T_b$. These results show that the optimization of the sampling offset is crucial when considering $\eta = 1$ sample per bit interval. We repeated this analysis at several OSNR values and verified that the observed behavior does not depend on the particular value of the OSNR.

We also evaluated the impact of the sampling epoch in a scenario with $\eta = 2$ equally spaced samples per bit interval. Our results show that the curves equivalent to those in Fig. 3 are flat. In other words, for a sampling rate equal to two samples per bit interval, the sensitivity on the sampling epoch is negligible. An interpretation of this result is that two samples per bit interval are approximately sufficient to satisfy with the considered filters the Nyquist condition on the minimum
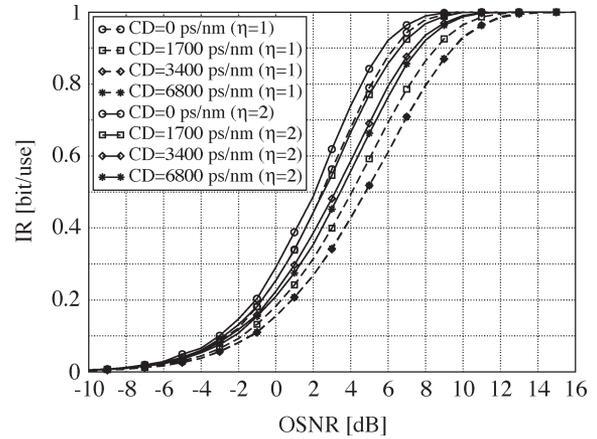
sampling frequency. In other words, the samples taken with an oversampling factor $\eta = 2$ carry enough information for accurate reconstruction of the time-continuous signal.

In Fig. 4, lower bounds on the IR are shown as functions of the OSNR for values of the sampling rate $\eta = 1$ and $\eta = 2$ samples per bit interval. Several values of the CD are considered. In the synchronous sampling case ($\eta = 1$), the sampling epoch is optimized for each OSNR and for each CD value. As expected, the IR tends to 1 for increasing OSNR, i.e., reliable transmission of 1 bit per channel use is possible for sufficiently large OSNR. However, for a fixed value of IR, an increasing OSNR penalty is incurred for higher values of CD. The influence of the CD on the IR will be discussed in detail in the next sections. Consider now the difference between $\eta = 1$ and $\eta = 2$ samples per bit interval for high IR values of interest in current optical communications (i.e., greater than 0.9). As one can see from Fig. 4, at CD equal to 0 ps/nm, the scheme with $\eta = 2$ exhibits a 0.5-dB gain with respect to that with synchronous sampling (i.e., $\eta = 1$). Moreover, for increasing values of CD, this gain increases further: for example, at 1700 ps/nm, the gain is about 1.8 dB.

The above results show that synchronous sampling is not sufficient to completely recover the information contained in the received (electrical) signal, and the choice of synchronous sampling can lead to an OSNR loss as high as 2 dB. An interpretation of this fact can be based on the following communication-theoretic considerations. Consider a linear channel such as a dispersive additive white Gaussian noise channel. It is well known that matched filtering followed by synchronous sampling produces an observable sequence that is a *sufficient statistic* for the detection of transmitted data [17]. In the case of a fiber-optic channel with direct photodetection, because of technological constraints, optical matched filtering is of no practical interest. As a consequence, due to the nonlinearity of the receiver, the synchronously sampled observable sequence is no longer a sufficient statistic for data detection. Linear electrical filtering does not guarantee optimal performance with synchronous sampling. This problem can be solved by increasing the sampling rate. Moreover, simple signal
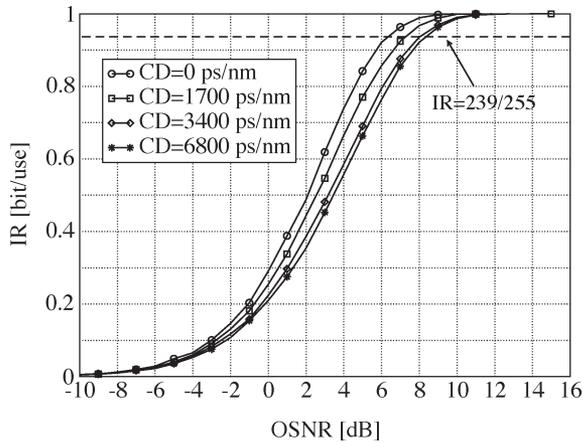
Fig. 5.   IR as a function of the OSNR in a scheme with NRZ OOK. Various values of CD are considered: 0, 1700, 3400, and 6800 ps/nm. The observables are represented with infinite precision (unquantized).

Fig. 6.   OSNR required to achieve an IR equal to 239/255 bit/use as a function of CD in an OOK transmission system. The dashed region is *achievable*.

processing considerations justify the fact that considering a sampling rate $\eta > 2$ should offer no advantage with respect to the case with $\eta = 2$. In the considered 10-Gb/s communication systems, the signal bandwidth at the output of the electrical filter is about 7 GHz. Therefore, the Nyquist rate is about 14 GHz. A sampling rate equal to $\eta = 2$ samples per bit interval corresponds to a sampling frequency equal to 20 GHz, which is above the Nyquist frequency and therefore sufficient to exactly represent the time-continuous observed signal.

Motivated by the above considerations, in the remaining part of this paper, the sampling rate will be set to $\eta = 2$ samples per bit interval. This choice allows to accurately predict the ultimate performance limits of EDC.

VII. Impact of CD and Quantization

In this section, we investigate the IR considering absence of quantization of the observables (this leads to a theoretical performance limit) and finite quantization considering a number of bits per observation sample ranging from 1 to 5. All IR values are obtained using the Monte Carlo simulation-based method described in Section III, and the number of transmitted bits is $n = 10^6$. As stated in Section VI, an oversampling factor $\eta = 2$ is considered, and the results are provided for both OOK and ODBM.

A. OOK Modulation

In this subsection, we investigate the IR performance of the optical transmission system described in Section V, where OOK with NRZ pulses is the used modulation format. In Fig. 5, IR is shown as a function of OSNR considering various values of CD: 0, 1700, 3400, and 6800 ps/nm, respectively. One can observe that increasing the value of CD causes an OSNR penalty that however seems to saturate for increasing values of CD. In fact, for the given IR, the OSNR penalty incurred when CD increases from 0 to 1700 ps/nm is about equal to that observed when CD increases from 1700 to 3400 ps/nm, whereas the OSNR penalty incurred when CD increases from
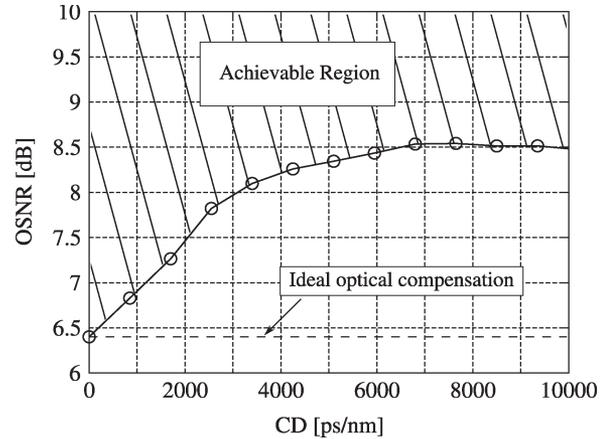
3400 to 6800 ps/nm is negligible. In order to better understand the impact of CD on system performance, we remark that in commercial optical communication systems, FEC codes are used to achieve virtually error-free performance. A typical code rate for optical FEC schemes using Reed–Solomon codes is 239/255, which means that for every 255 transmitted bits, only 239 represent the information payload, and the remaining 16 are redundant bits used for error detection and correction. Assuming that the code rate is set to 239/255, and keeping in mind that IR represents the maximum achievable reliable data transfer rate, it is possible to compute the OSNR needed to achieve the IR 239/255 as a function of the uncompensated CD. This can be pursued by obtaining the OSNRs of the intersections of a horizontal line at an IR equal to 239/255, shown in Fig. 5 as a dashed line, and the IR curves.

In Fig. 6, the OSNR needed to achieve an IR equal to 239/255 is shown as a function of CD. Since the IR is an increasing function of the OSNR, the whole (dashed) region above the curve in Fig. 6 represents the set of (OSNR,CD) pairs that can be reliably achieved (with error probability as low as desired) by properly designed and sufficiently complex transmission schemes. In other words, the dashed region is *achievable*. One can observe the predicted behavior: the OSNR starts at 6.5 dB, increases in the CD range between 0 and 3000 ps/nm, and then settles in the neighborhood of 8.5 dB, at which it seems to remain stable in the high-CD region. Note that since all the IR curves previously shown are lower bounds for the actual IR, the OSNR curve in Fig. 6 (and in the following figures) is an upper bound on the actual OSNR. This guarantees the achievability of the dashed region. If ideal optical CD compensation at the receiver could be achieved, it would be possible to set the system operating point to the CD value corresponding to the lowest possible OSNR, which in this case is CD equal to 0 ps/nm. As a consequence, with ideal optical CD compensation at the receiver, the performance does not depend on the CD value. This is shown in Fig. 6, where the horizontal dashed line represents an upper bound on the OSNR curve for the considered OOK system with ideal optical compensation at the receiver.

We now focus our attention on the impact of quantization of the observables on the IR. In this paper, we consider only *uniform* quantization, i.e., the thresholds describing the quantization function are equally spaced. If the number of bits representing the quantized value is m, then 2^m regions are considered and correspondingly $2^m - 1$ thresholds. A uniform quantization function is uniquely identified by: 1) the number of bits m; 2) the maximum threshold; and 3) the minimum threshold. If we denote the quantized interval to which the observable $y_k^{(i)}$ belongs by an index $z_k^{(i)}$, and, as a consequence, the quantized vector observable by $\boldsymbol{z}_k = (z_k^{(0)}, \ldots, z_k^{(\eta-1)})$, the IR computation algorithm described in Section III can still be used after a formal substitution of $y_k^{(i)}$ with $z_k^{(i)}$ and $\boldsymbol{y}_k$ with $\boldsymbol{z}_k$. In particular, since we consider $\gamma = 0$, (11) becomes

$$p\left(\boldsymbol{z}_k | \boldsymbol{z}_{k-\gamma}^{k-1}, \boldsymbol{a}_{k-L}^k\right) = \prod_{i=0}^{\eta-1} p\left(z_k^{(i)} | \boldsymbol{a}_{k-L}^k\right) \qquad (14)$$

where the conditional probability mass function $p(z_k^{(i)} | \boldsymbol{a}_{k-L}^k)$ is obtained as

$$p\left(z_k^{(i)} | \boldsymbol{a}_{k-L}^k\right) = P\left\{y_k^{(i)} \in \mathcal{I}\left(z_k^{(i)}\right) | \boldsymbol{a}_{k-L}^k\right\}$$

$$= \int_{\mathcal{I}\left(z_k^{(i)}\right)} p\left(y_k^{(i)} | \boldsymbol{a}_{k-L}^k\right) dy_k^{(i)} \qquad (15)$$

where $\mathcal{I}(z_k^{(i)})$ denotes the quantization interval in correspondence with the index $z_k^{(i)}$, and $p(y_k^{(i)} | \boldsymbol{a}_{k-L}^k)$ is obtained as described in Section IV.

In order to avoid information loss, the quantized signal must be representative of the statistics of the received signal. As a consequence, the maximum and minimum thresholds must be optimized as functions of every parameter affecting the received signal, namely the OSNR and the CD (since every other parameter, e.g., the bandwidths of the various filters, is assumed to be a design constraint). In the following results and throughout the remainder of this paper, the minimum and maximum thresholds are optimized for every value of OSNR and CD.

In Fig. 7, the lower bound on the IR of an NRZ OOK scheme is shown as a function of the OSNR for CD equal to 1700 ps/nm. Various levels of quantization with 1, 2, and 3 bits per sample, as well as absence of quantization, are considered. One can observe the expected behavior: as the number of quantization bits increases, the distance between quantized and unquantized IR curves tends to zero. Moreover, while the 1-bit IR curve exhibits a quantization loss (in terms of OSNR) of about 2 dB, the 2-bit IR curve is characterized by a quantization loss of only 0.2 dB. The 3-bit IR curve exhibits a negligible quantization loss.

In Fig. 8, the upper bound on the OSNR required to achieve an IR equal to 239/255 bit/use is shown as a function of CD for $\eta = 2$ samples per bit interval. The performance with no quantization and 1-bit, 2-bit, and 3-bit uniform quantization is analyzed. One can immediately recognize that 1-bit quantiza-
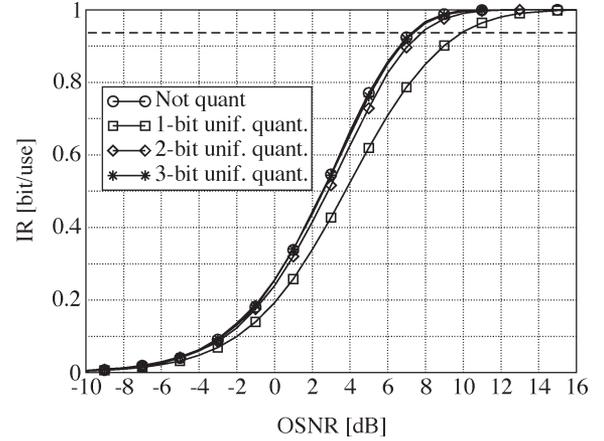
Fig. 7. IR as a function of OSNR at a dispersion value of 1700 ps/nm for an NRZ OOK scheme. Quantization levels of 1, 2, and 3 bits/sample and no quantization are considered.
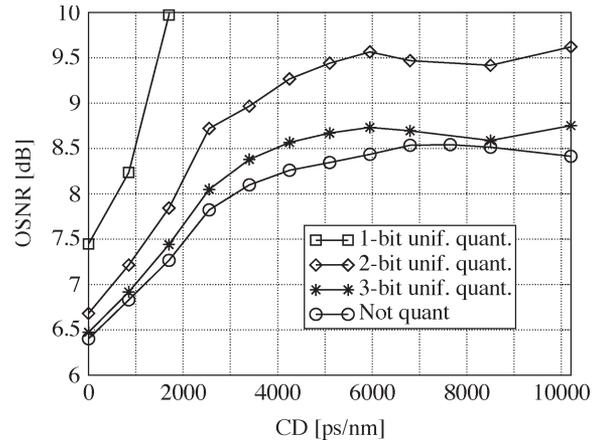
Fig. 8. OSNR as a function of CD at an IR equal to 239/255 bit/use for various quantization levels. An NRZ OOK scheme with oversampling factor $\eta = 2$ is considered.

tion does not allow effective data transfer, since a very high OSNR is needed to recover even a CD equal to 2000 ps/nm. The 2-bit OSNR curve shows instead that this quantization level is sufficient to recover from high-dispersion values. Nevertheless, a 2-bit quantization causes a penalty of approximately 1 dB with respect to the unquantized case in the high-dispersion region. On the other hand, it is easily recognized that a 3-bit quantization is sufficient to accurately represent the received sampled signal, since this induces a penalty that ranges between about 0.1 dB (in B2B) and about 0.3 dB (in the medium CD region).

In Fig. 9, the upper bound on the OSNR required to achieve an IR equal to 239/255 bits per channel use is shown, as a function of the number of quantization bits, considering several CD values. One can observe that the highest relative performance improvement is obtained by increasing the number of quantization bits from 1 to 2. On the other hand, a 4- or 5-bit quantization is needed in order to recover the entire information content embedded into the received signal. This is especially true in the case of medium/high values of CD.
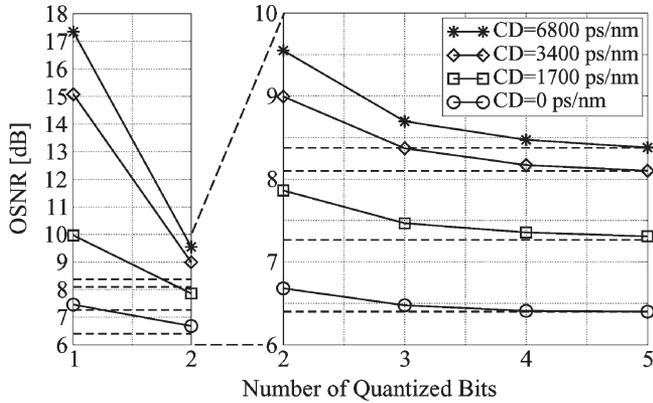
Fig. 9.   OSNR for an NRZ OOK scheme as a function of the number of quantization bits at an IR equal to 239/255. Various values of CD, namely 0, 1700, 3400, and 6800 ps/nm, are considered.
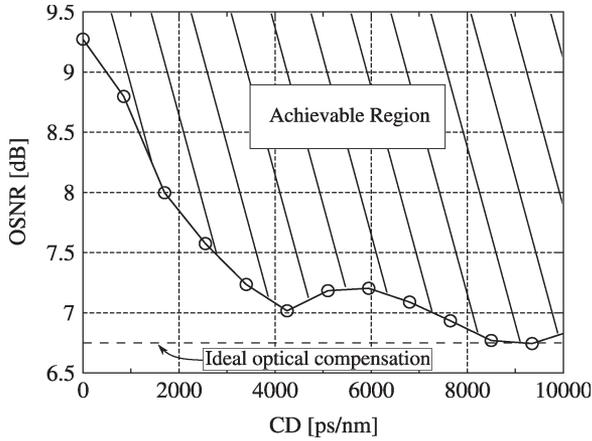
Fig. 10.   OSNR as a function of CD at an IR equal to 239/255 bit/use for an ODBM transmission scheme.

B. ODBM

In this section, the IR of the ODBM transmission scheme described in Section V is investigated. The IR curves as functions of the OSNR are similar to the IR curves in the OOK case. Nevertheless, the relationship between IR and CD is not monotone anymore. In Fig. 10, an upper bound on the OSNR required to achieve an IR equal to 239/255 bit/use is shown as a function of CD considering $\eta = 2$ samples per bit interval and no quantization of the received signal. As for OOK, the dashed area indicates the *achievable* region. In other words, any (OSNR,CD) pair of values in this region can be achieved reliably (i.e., with error probability as low as desired) by using carefully designed and sufficiently complex EDC systems. By examining the results in Fig. 10, one can better understand the inherent difference between OOK and ODBM. In fact, unlike OOK systems, the performance of ODBM systems improves for increasing values of CD. In particular, the OSNR required to achieve reliable transmission at 9200 ps/nm is 6.73 dB. Moreover, the ODBM performance (in terms of required OSNR for a target IR) in the medium/high-CD region is slightly dependent on CD. If ideal optical CD compensation at the receiver is considered, the obtained results suggest that the optimum operating point is about 9000 ps/nm. An upper bound to the
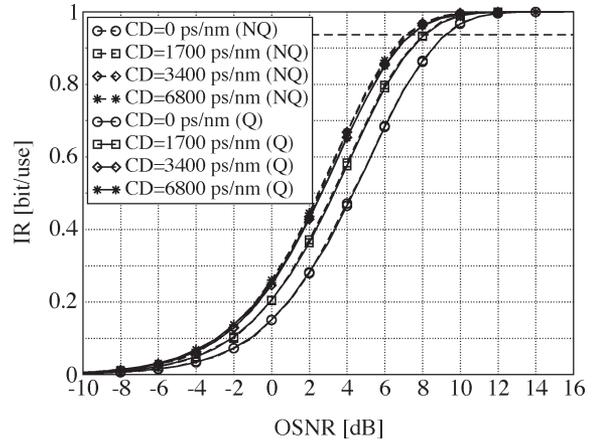
Fig. 11.   IR as a function of OSNR at dispersion values of 0, 1700, 3400, and 6800 ps/nm for an ODBM scheme. In each case, the IR with 3-bit quantization (Q) and without quantization (NQ) is shown.
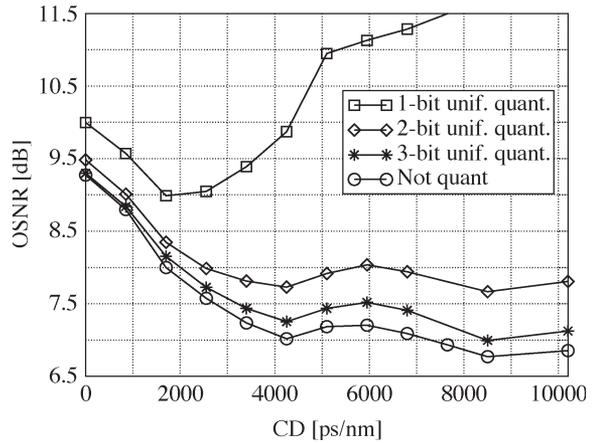
Fig. 12.   OSNR versus dispersion at an IR equal to 239/255 bit/use for a ODBM transmission scheme. Various quantization levels are considered: 1-bit, 2-bit, and 3-bit quantization and no quantization.

OSNR curve with ideal optical CD compensation is shown in Fig. 10 as a dashed horizontal line.

Let us now evaluate a lower bound on the IR as a function of the OSNR for values of CD from 0 to 6800 ps/nm in the absence of quantization and in the presence of uniform 3-bit quantization of the output signal. The corresponding results are shown in Fig. 11. The behavior of OOK schemes in the presence of quantization is confirmed for ODBM schemes as well. In particular, the results in Fig. 11 show that a quantization level of 3 bits per sample is sufficient to almost completely recover the information embedded in the unquantized observables. In fact, the distance between unquantized and 3-bit quantized curves in terms of OSNR is less than 0.2 dB.

In Fig. 12, the upper bound on the OSNR required to achieve an IR equal to 239/255 in ODBM schemes is shown as a function of CD. The performance with no quantization and uniform quantization is evaluated. In the quantized case, one, two, and three quantization bits are considered. As expected, the behavior characterizing the OOK scenario is confirmed in the ODBM schemes as well. In fact, although a 1-bit quantization exhibits a significant loss (with respect to high-level

quantization schemes), in the ODBM case, data transmission with acceptable performance is still possible at dispersion values as high as 6000 ps/nm. The IR curve for 2-bit quantization shows an asymptotic (for high values of the CD) penalty of about 1 dB as in the OOK case, whereas the IR curve with 3-bit quantization has an asymptotic penalty lower than 0.35 dB, which is in excellent agreement with the OOK case.

VIII. DISCUSSION

The results presented in the previous sections give an overview of the intrinsic potential of electronic signal processing in optical transmission schemes affected by severe uncompensated CD. In particular, in the case of OOK, the high-dispersion region is characterized by an unavoidable loss with respect to the B2B scenario of about 2 dB. Given sufficiently complex processing, the obtained results suggest that it is possible to mitigate the effects of significant dispersion. In fact, it has been shown that an OSNR equal to 8.5 dB is in principle sufficient to achieve error-free performance at high values of CD. Moreover, the shape of the OSNR curve in the OOK case in Fig. 8 seems to suggest that even higher values of CD (beyond 10 000 ps/nm) would not require a further significant increase of OSNR, i.e., a saturation phenomenon seems to appear. The obtained results indicate that a 3-bit quantization level is sufficient to almost completely recover the inherent loss due to quantization.

In the case of ODBM, our information-theoretic results confirm the well-known high-CD tolerance of this modulation format. Moreover, in the high-CD region, ODBM schemes exhibit a performance similar to that of OOK schemes in B2B.

The length of the sequence (i.e., 10^6 bits) used for each IR evaluation has been chosen in order to obtain numerical convergence and make the confidence interval sufficiently small. At this point, the following two remarks are worthwhile.

1) The obtained IR curves represent *lower bounds* on the actual IR. In fact, the adopted channel model assumes conditional independence of the observables, whereas a small (but positive) correlation characterizes the actual observables. As a consequence, the highlighted achievable regions (in Figs. 8 and 12) are part of potentially wider achievable regions. In fact, exact evaluation of the IR might extend the achievable regions toward low OSNR values. This extension is expected to be very limited due to the fact that the correlation between consecutive observables has been experimentally found to be small. This research direction is currently being further pursued.

2) Although it is true that the (OSNR,CD) pairs in the achievable regions in Figs. 8 and 12 can be achieved by practical transmission schemes, the complexity of such schemes could be challenging, especially in the high-CD region, where the system memory is very large and optimal decision strategies such as MLSD are too complex to be practically feasible.

Although this IR-based analysis provides theoretical performance limits, several recently proposed design techniques allow to approach these limits in many practical scenarios. In particular, the use of powerful error correcting codes and iterative decoding techniques can be an appealing solution for future advanced optical communication schemes [35], [36].

IX. CONCLUDING REMARKS

In this paper, the ultimate performance limits of electronic signal processing for optical transmission schemes affected by CD have been investigated by numerical evaluation of lower bounds on the IR. OOK with NRZ pulses and ODBM transmission schemes have been considered. The obtained results show that an unavoidable asymptotic *loss* with respect to the B2B case of about 2 dB characterizes the considered OOK schemes for large values of CD. In the ODBM case, instead, there is an asymptotic *gain* with respect to B2B of approximately 2.5 dB at large CD values. In all cases, the use of electronic signal processing holds a great potential: for OOK, error-free performance can be achieved at OSNR values between 6.5 and 8.5 dB for dispersion values ranging from 0 to 10 000 ps/nm; for ODBM, error-free performance is obtainable for OSNR values between 9.3 and 6.73 dB for dispersion ranging from 0 to 10 000 ps/nm. The impact of the quantization level of the observables has been investigated, showing that 1-bit quantization leads to an unacceptable performance loss, whereas a quantization level with at least 3 bits per sample is sufficient to practically achieve the same performance of unquantized schemes. Moreover, our information-theoretic analysis shows that a sampling rate of two samples per bit interval is needed in order to fully exploit the information embedded in the received electrical signal. This is in good agreement with previous results based on the bit error rate analysis [11].

Finally, we wish to remark that the techniques used in this paper can be used to characterize nonlinear fiber effects as well. This is a subject of current research activity.

REFERENCES

[1] G. Agrawal, *Fiber-Optic Communications Systems*. New York: Wiley, 2002.

[2] J. H. Winters and R. D. Gitlin, "Signal processing techniques in long-haul fiber-optic systems," *IEEE Trans. Commun.*, vol. 38, no. 9, pp. 1439–1453, Sep. 1990.

[3] H. Bülow, "Electronic equalization of transmission impairments," in *Proc. OFC Conf.*, Anaheim, CA, Mar. 2002, pp. 24–25.

[4] V. Curri, R. Gaudino, A. Napoli, and P. Poggiolini, "Electronic equalization for advanced modulation formats in dispersion-limited systems," *IEEE Photon. Technol. Lett.*, vol. 16, no. 11, pp. 2556–2558, Nov. 2004.

[5] C. Xia and W. Rosenkranz, "Performance enhancement for duobinary modulation through nonlinear electrical equalization," in *Proc. ECOC*, Glasgow, U.K., Sep. 2005, vol. 2, pp. 255–256.

[6] O. E. Agazzi, M. R. Hueda, H. S. Carrer, and D. E. Crivelli, "Maximum-likelihood sequence estimation in dispersive optical channels," *J. Lightw. Technol.*, vol. 23, no. 2, pp. 749–763, Feb. 2005.

[7] H. S. Carrer, D. E. Crivelli, and M. R. Hueda, "Maximum likelihood sequence estimation receivers for DWDM lightwave systems," in *Proc. IEEE GLOBECOM*, Dallas, TX, Dec. 2004, pp. 1005–1010.

[8] H. S. Carrer, M. R. Hueda, and D. E. Crivelli, "MLSE-based receivers on DWDM lightwave systems," in *Proc. 9th ICCS*, Singapore, Sep. 2004, pp. 573–578.

[9] D. E. Crivelli, H. S. Carrer, and M. R. Hueda, "On the performance of reduced-state Viterbi receivers in IM/DD optical transmission systems," in *Proc. ECOC*, Stockholm, Sweden, Sep. 2004, pp. 634–635.

[10] G. Bosco and P. Poggiolini, "Long-distance effectiveness of MLSE IMDD receivers," *IEEE Photon. Technol. Lett.*, vol. 18, no. 9, pp. 1037–1039, May 2006.

[11] T. Foggi, E. Forestieri, G. Colavolpe, and G. Prati, "Maximum likelihood sequence detection with closed-form metrics in OOK optical systems impaired by GVD and PMD," *J. Lightw. Technol.*, vol. 24, no. 8, pp. 3073–3087, Aug. 2006.

[12] T. M. Cover and J. A. Thomas, *Elements of Information Theory*. New York: Wiley, 1991.

[13] D. Arnold and H.-A. Loeliger, "On the information rate of binary-input channels with memory," in *Proc. IEEE ICC*, Helsinki, Finland, Jun. 2001, pp. 2692–2695.

[14] V. Sharma and S. K. Singh, "Entropy and channel capacity in the regenerative setup with applications to Markov channels," in *Proc. IEEE ISIT*, Washington, DC, Jun. 2001, p. 283.

[15] H. D. Pfister, J. B. Soriaga, and P. H. Siegel, "On the achievable information rates of finite state ISI channels," in *Proc. GLOBECOM*, San Antonio, TX, Nov. 2001, pp. 2992–2996.

[16] D. Arnold, H. A. Loeliger, P. O. Vontobel, A. Kavcic, and W. Zen, "Simulation-based computation of information rates for channel with memory," *IEEE Trans. Inf. Theory*, vol. 52, no. 8, pp. 3498–3508, Aug. 2006.

[17] K. Yonenaga and S. Kuwano, "Dispersion-tolerant optical transmission system using duobinary transmitter and binary receiver," *J. Lightw. Technol.*, vol. 15, no. 8, pp. 1530–1537, Aug. 1997.

[18] J. Tang, "The Shannon channel capacity of dispersion-free nonlinear optical fiber transmission," *J. Lightw. Technol.*, vol. 19, no. 8, pp. 1104–1109, Aug. 2001.

[19] E. E. Narimanov and P. Mitra, "The channel capacity of a fiber optics communication system: Perturbation theory," *J. Lightw. Technol.*, vol. 20, no. 3, pp. 530–537, Mar. 2002.

[20] J. Tang, "A comparison study of the Shannon channel capacity of various nonlinear optical fibers," *J. Lightw. Technol.*, vol. 24, no. 5, pp. 2070–2075, May 2006.

[21] S. Shamai, "On the capacity of a direct-detection photon channel with intertransition-constrained binary input," *IEEE Trans. Inf. Theory*, vol. 37, no. 6, pp. 1540–1550, Nov. 1991.

[22] J. Li, "On the achievable information rate of asymmetric optical fiber channels with amplifier spontaneous emission noise," in *Proc. IEEE MILCOM*, Boston, MA, Oct. 2003, pp. 124–129.

[23] C. Berrou and A. Glavieux, "Near optimum error correcting coding and decoding: Turbo-codes," *IEEE Trans. Commun.*, vol. 44, no. 10, pp. 1261–1271, Oct. 1996.

[24] I. B. Djordjevic, B. Vasic, M. Ivkovic, and I. Gabitov, "Achievable information rates for high-speed long-haul optical transmission," *J. Lightw. Technol.*, vol. 23, no. 11, pp. 3755–3763, Nov. 2005.

[25] E. Forestieri, "Evaluating the error probability in lightwave systems with chromatic dispersion, arbitrary pulse shape and pre- and postdetection filtering," *J. Lightw. Technol.*, vol. 18, no. 11, pp. 1493–1503, Nov. 2000.

[26] R. Ramaswami and K. Sivarajan, *Optical Networks*. San Francisco, CA: Morgan Kaufman, 2001.

[27] M. Franceschini, G. Ferrari, R. Raheli, and G. Bongiorni, "Fundamental limits of electronic dispersion compensation in optical communications with direct photodetection," *Electron. Lett.*, vol. 42, no. 15, pp. 874–875, Jul. 20, 2006.

[28] P. J. Winzer and R. Essiambre, "Advanced optical modulation formats," *Proc. IEEE*, vol. 94, no. 5, pp. 952–985, May 2006.

[29] J. G. Proakis, *Digital Communications*, 4th ed. New York: McGraw-Hill, 2001.

[30] G. Ferrari, G. Colavolpe, and R. Raheli, "A unified framework for finite-memory detection," *IEEE J. Sel. Areas Commun.*, vol. 23, no. 9, pp. 1697–1706, Sep. 2005.

[31] S. M. Ross, *Stochastic Processes*. New York: Wiley, 1983.

[32] L. R. Bahl, J. Cocke, F. Jelinek, and J. Raviv, "Optimal decoding of linear codes for minimizing symbol error rate," *IEEE Trans. Inf. Theory*, vol. IT-20, no. 2, pp. 284–287, Mar. 1974.

[33] E. W. Weistein, "Levenberg–Marquardt method," *From MathWorld—A Wolfram Web Resource*. [Online]. Available: http://mathworld.wolfram.com/Levenberg-MarquardtMethod.html

[34] M. R. Hueda, D. E. Crivelli, and H. S. Carrer, "Performance of MLSE-based receivers in lightwave systems with nonlinear dispersion and amplified spontaneous emission noise," in *Proc. IEEE GLOBECOM*, Dallas, TX, Dec. 2004, pp. 299–303.

[35] C. Douillard, M. Jezequel, C. Berrou, A. Picart, P. Didier, and A. Glavieux, "Iterative correction of intersymbol interference: Turbo-equalization," *Eur. Trans. Telecommun.*, vol. 6, no. 5, pp. 507–511, Sep./Oct. 1995.

[36] M. Jager, T. Rankl, J. Speidel, H. Bulow, and F. Buchali, "Performance of turbo equalizers for optical PMD channels," *J. Lightw. Technol.*, vol. 24, no. 3, pp. 1226–1236, Mar. 2006.

Michele Franceschini was born in Milan, Italy, in 1977. He received the Dr. Ing. (Laurea, five-year program) degree (*summa cum laude*) in electrical engineering and Ph.D. degree from the University of Parma, Parma, Italy, in 2002 and 2006, respectively.

He currently holds a postdoc position at the University of Parma. His research interests lie in the area of communication and information theory with particular emphasis on low-density parity check code design, theoretical aspects of optical communication, advanced signal processing techniques, synchronization, and low-complexity implementation of digital communication systems.

Dr. Franceschini received the Paolo Conti Award as the best graduate in information engineering at the University of Parma in the academic year 2002.

Giorgio Bongiorni was born in Codogno, Italy, on March 27, 1981. He received the M.S. degree (*summa cum laude*) in telecommunications engineering from the University of Parma, Parma, Italy, in 2006.

From May 2006 to April 2007, he was with the University of Parma under a post-degree grant on "transmission techniques over optical fiber" in collaboration with Cisco Systems. He is now with Selta S.p.A., Roveleto di Cadeo, Piacenza (PC), Italy. His main research interests include digital and optical transmission and information theory.

Gianluigi Ferrari (S'97–M'03) was born in Parma, Italy, in November 1974. He received the Laurea degree (five-year program, *summa cum laude*) and Ph.D. degree in electrical engineering from the University of Parma, Parma, in 1998 and 2002, respectively.

From July 2000 to December 2001, he was a Visiting Scholar at the Communication Sciences Institute, University of Southern California, Los Angeles. Since 2002, he has been a Research Professor in the Department of Information Engineering, University of Parma, where he is currently the Coordinator of the Wireless *Ad-hoc* and Sensor Networks (WASN) Laboratory. Between 2002 and 2004, he visited several times, as a Research Associate, the Electrical and Computer Engineering Department, Carnegie Mellon University, Pittsburgh, PA. He has published more than 70 papers in leading international conferences and journals. He is coauthor of *Detection Algorithms for Wireless Communications, with Applications to Wired and Storage Systems* (Wiley, 2004), *Teoria della probabilità e variabili aleatorie conapplicazioni* (McGraw-Hill, 2005), and *Ad Hoc Wireless Networks: A Communication-Theoretic Perspective* (Wiley, 2006). His research interests include digital communication systems design, *ad hoc* wireless networking, adaptive signal processing (with particular emphasis on iterative detection techniques for channels with memory), and information theory.

Dr. Ferrari acts as a frequent reviewer for many international journals and conference proceedings. He also acts as a Technical Program member for several international conferences. He is a corecipient of a Best Student Paper Award at the 2006 International Workshop on Wireless Ad hoc Networks (IWWAN'06). Since 2007, he has been on the Editorial Board of the *The Open Electrical and Electronic Engineering Journal*, Bentham Publishers.

Riccardo Raheli (M'87) received the Dr. Ing. (Laurea) degree (*summa cum laude*) in electrical engineering from the University of Pisa, Pisa, Italy, in 1983, the M.S. degree in electrical and computer engineering from the University of Massachusetts, Amherst, in 1986, and the Ph.D. (Perfezionamento) degree (*summa cum laude*) in electrical engineering from the Scuola Superiore di Studi Universitari e di Perfezionamento (now "S. Anna"), Pisa, in 1987.

From 1986 to 1988, he was with Siemens Telecomunicazioni, Cassina de' Pecchi, Milan, Italy. From 1988 to 1991, he was a Research Professor at Scuola Superiore di Studi Universitari e di Perfezionamento. In 1990, he was a Visiting Assistant Professor at the University of Southern California, Los Angeles. Since 1991, he has been with the University of Parma, Parma, Italy, where he is currently a Professor of communications engineering. His research work has lead to numerous scientific publications in leading international journals and conference proceedings as well as a few industrial patents. In 1990, he conceived (with A. Polydoros) the principle of *per-survivor processing*. He is the coauthor of *Detection Algorithms for Wireless Communications, with Applications to Wired and Storage Systems* (Wiley, 2004). Since 2003, he has been on the Editorial Board of the European *Transactions on Telecommunications* as Editor for communication theory. His scientific interests are in the general area of statistical communication theory with application to wireless, wired, and storage systems, and special attention to data detection in uncertain environments, iterative information processing, and adaptive algorithms for communications.

Dr. Raheli served on the Editorial Board of the IEEE TRANSACTIONS ON COMMUNICATIONS as Editor for detection, equalization, and coding from 1999 to 2003. He also served as Guest Editor of the IEEE JOURNAL ON SELECTED AREAS IN COMMUNICATIONS, "Special Issue on Differential and Noncoherent Wireless Communications," published in September 2005.

Fausto Meli was born in Piacenza, Italy, in 1956. He received the Doctorate degree in nuclear engineering (optoelectronic specialization) from the Politecnico di Milano, Milan, Italy, in 1981.

In 1983, was with Pirelli Cavi e Sistemi R&D Laboratory, where he worked in the area of new optical fiber development and characterization. In 1989, he was involved in a joint research program on optical amplification with University of Southampton, Southampton, U.K., where he later became responsible for optical development for Pirelli Optical Systems contributing to the design of the first field-deployed optically amplified system and the first and next-generation DWDM optical systems. In the same period, he was also engaged in EC projects like RACE II/Multi Wavelength Transport Network (MWTN) and ACTS/Fluoro-aluminate Amplifier for Second Telecom Window (FAST). Since 2000, he has been with Cisco Photonics, Monza, Italy, as a result of Pirelli Optical Systems acquisition by Cisco Systems, where he was responsible for the Optical Development and Advanced Technology Teams. He was the coauthor of more than 45 international patents filed and of several scientific journals and conference papers in the different fields covered. During the last two years, as part of the engineering technical staff, he was involved on future technology developments for optical systems and leading the optical network design support activity.

Andrea Castoldi was born in Monza, Italy, on November 24, 1969. He received the Laurea (M.S.) degree in physics from the Universita' Statale degli Studi di Milano, Milano, Italy, in 1995.

From 1995 to 1999, he was a Designer of integrated optical components at Pirelli Optical Systems. Since 2000, he has been an Optical Designer at Cisco Photonics, Monza, where he is working in the field of fiber nonlinearities for optical network planning. He is the author of four patents on optical components technology.